EIR-Bericht Nr. 304

Eidg. Institut für Reaktorforschung Würenlingen
Schweiz

Gas Cooled Fast Breeder Reactors Using Mixed Carbide Fuel

S. Kypreos

Würenlingen, September 1976

EIR-Bericht Nr. 304

Gas Cooled Fast Breeder Reactors Using Mixed Carbide Fuel

S. Kypreos

Würenlingen, September 1976

Contents

	page
Introduction	1
Methods used in the calculation of core thermohydraulics and physics design: General description	3
Core thermohydraulic analysis: Parametric study	4
Pin diameter	7
Core pressure drop	10
Core active height	11
Maximum cladding temperature	13
Maximum fuel centerline temperature	15
Comparative studies of mixed carbide versus mixed oxide fuel using the fuel management program GAUGEFM: Neutronic analysis and fuel cycle cost	17
Conclusions	23
Final remarks	23
Literature	25
Appendix A: Core thermohydraulics and neutronic calculations	26
Mean value of conductivity	29
Core pressure drop	30
Core dimensions	31
Neutronic model	31
Appendix B: Spectrum calculations	34

Introduction

The fast reactors being developed at the present time use mixed oxide fuel, stainless-steel cladding and liquid sodium as coolant (LMFBR). Theoretical and experimental designing work has also been done in the field of gas-cooled fast breeder reactors.

Although the world wide efforts to solve the energy and resource conservation problem are devoted mainly to the LMFBR concept, (SNR, PFR, PHENIX, FFTF, etc.) its breeding performance is questionable due to the simultaneous negative development in several areas. Stainless steel swelling at high neutron fluence, errors in cross-section libraries and lower allowable linear power ratings have resulted in compound doubling times of 25 years. This breeding performance is insufficient.

Although every effort is being made to improve the present design using advanced oxide fuel the doubling time is not expected to be lower than 15 years.

The more advanced carbide fuel offers greater potential for developing fuel systems with doubling times in the range of ten years (1). A better breeding performance could be obtained due to the higher heavy metal density of mixed carbide, while its higher thermal conductivity (see Fig. 1) allows high linear ratings with reduced fissile material inventory and compact core designs.

The situation with GCFRs is more encouraging than with LMFBRs, using present mixed oxide technology. A GCFR system is based on LMFBR fuel and physics development and on HTGR technology such as the PCRV, the helium circulator and steam generator. Helium has several advantages over sodium; it is chemically inert; it does not change phase; it does not become radioactive and it does not moderate the neutrons thus leading to high breeding gain and small void coefficient.

Fig. 1 Oxide and carbide fuel thermal conductivity

$K_O = 1.1 + \frac{100}{.08227\ T\ (^oC)}$ (w/m°C)

90% theor. density of (U-Pu) O_2

$K_C = 8.5 + 2.88 \cdot 10^{-3}\ T\ (^oC)$ (w/m°C)

80 % theor. density of (U-Pu)C

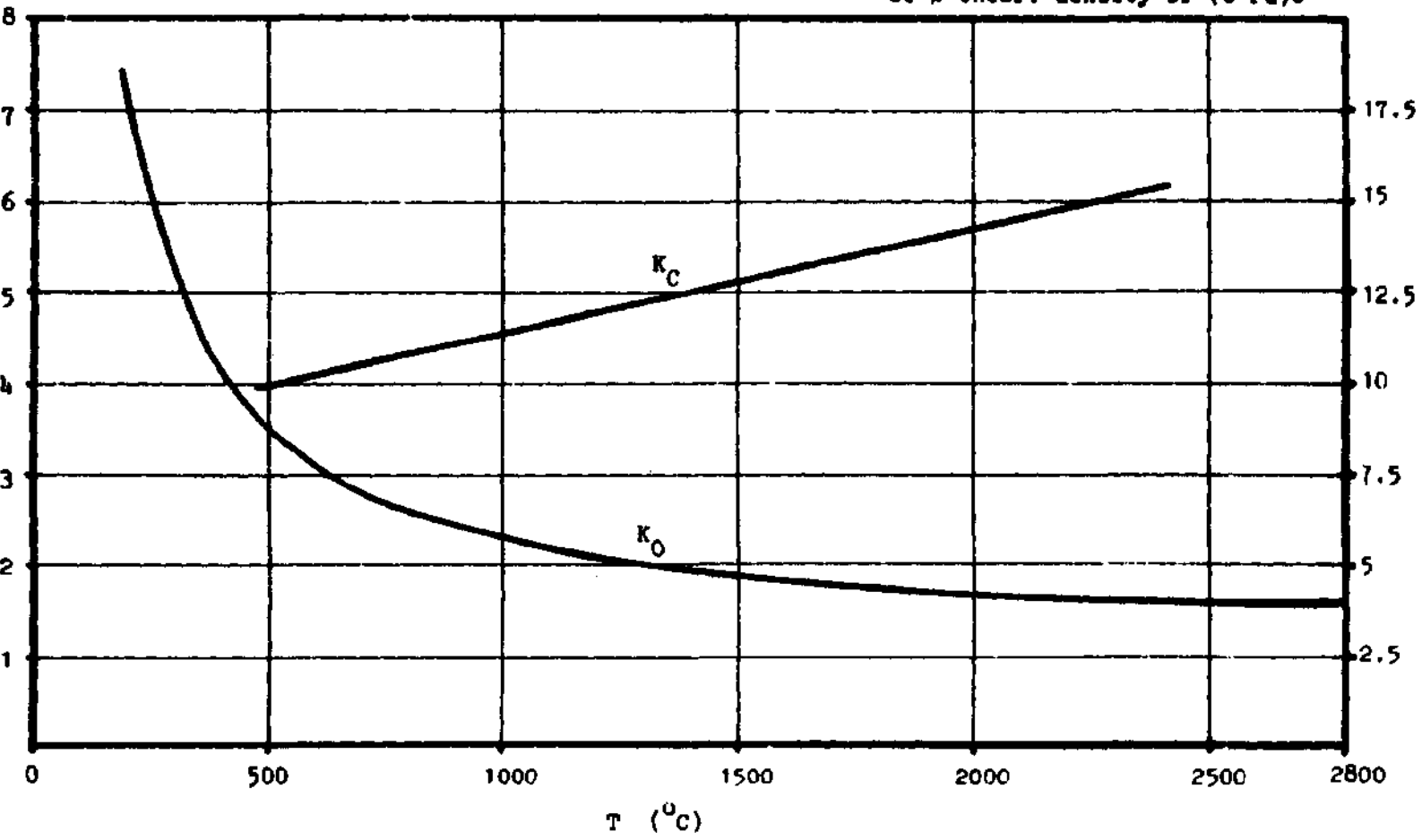

Although sodium has a better heat transfer coefficient and works at low pressures, extended theoretical and experimental work has shown that the heat transfer characteristics of helium under typical fast breeder operating conditions are adequate.

The carbide fuel, when its technology is available, would be beneficial to the LMFBR's, since it is better fitted to the cooling capabilities of sodium and improves breeding ratio.

Our study is an effort to assess the thermohydraulic and physics performance of a GCFR utilising this fuel.

The question to be answered is whether the helium is an efficient coolant to be coupled with the advanced carbide fuel while preserving its superior neutronic performance. Also an assessment of the fuel cycle cost in comparison to oxide fuel will be presented.

Methods used in the calculation of core thermohydraulics and physics design ; General description :

Subroutine REGA computes the maximum thermal power produced for a central channel and determines the required coolant mass flow such that the fuel centerline and outside cladding wall temperature reach their specified limits for a desired core pressure drop.

The core geometry is specified from the assumed axial and radial form factors. A simplified two dimensional neutronics model with a self-contained cross-section library calculates the fissile enrichments and its distribution in the core zones to achieve a critical system with equal power peaks in radial direction. Iterations between the assumed and calculated power factors follow.

The results of the simplified neutronics model are used as a first guess to initiate the physics calculation with the two dimensional multi-group program GAUGEFM (2).

This program performs the following functions:

- Re-adjusts the initial loadings normalising the power profile and taking into account the reactivity losses due to burn-up.

- Specifies the fuel residence time according to the damage fluence constraint.

- Performs fuel management operations and fuel cycle cost calculations using the present worth method (3).

The above described procedure is explained in details in Appendix A.

Core thermohydraulic analysis;
Parametric study:

The most important constraints in determining the core design and plant lay-out are the maximum allowable cladding temperature, fast fluence and the maximum fuel temperature.

Higher cladding temperature means generally higher coolant core exit temperature and consequently higher plant efficiency and reduced heat exchanger surface.

Higher fuel temperatures result in higher linear power rating and require better thermal conductivities as offered by carbide fuels.

Also a higher allowable neutron fluence for the cladding increases the fuel residence time thus decreasing the fuel cycle costs.

One of the near term goals for the advanced breeder development program in the USA is the research for improved cladding and subassembly duct material that can withstand neutron exposures up to $2.5 \cdot 10^{23}$ nvt (E>.1 MeV) with total swelling < 5 %. From this development every breeder concept can profit. Since at the present time the limits on maximum allowable fuel and cladding temperatures and fast fluence are not yet established, some reasonable values should be selected.

A few parameters have been varied in the study, such as: pin diameter and length, core pressure drop, maximum fuel centre line temperature (or maximum linear power rating) and maximum cladding temperature. The permissible fluence limit has also been changed in the fuel cycle cost analysis.

The designs studied follow the general principles of the GCFR demo plant proposed by GA, as far as the fuel pin and the fuel element geometry is concerned.

The plant efficiency corresponds to an indirect steam cycle with steam to steam reheater, while the secondary cycle conditions are not optimised.

The proposed GA demo plant is using gas to steam reheating after expansion in the blower turbine. This increases the plant efficiency by three percentage points with complicated steam flow paths and increased capital expenses. The gas to steam reheating could have decrease the calculated core dimensions and critical masses by 10 %.

A set of efficiency calculations was done and the results where fitted to the core thermohydraulics subroutine. Fig. 2 gives the calculated efficiency as a function of the core outlet temperature.

Fig. 2

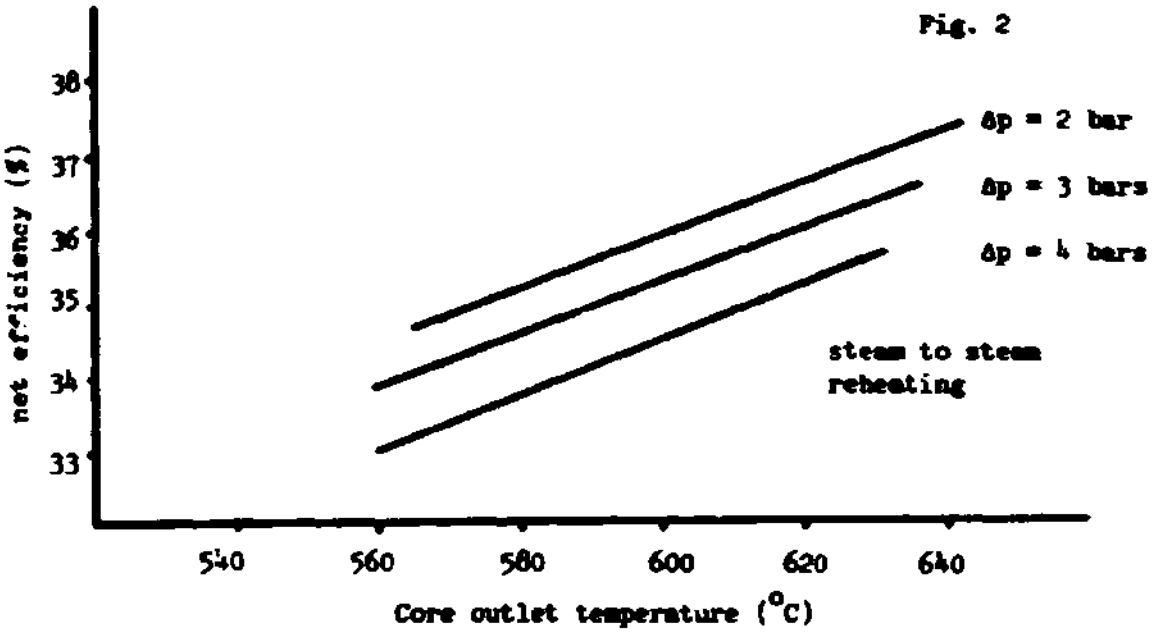

Plant efficiency as a function of core outlet temperature and pressure drop, T_{inlet} = 280 °C, Pressure at core inlet = 90 bar

The fuel elements have 270 pins which use the vented fuel concept while in 30 fuel elements enough space has been left to position the control rods. Three fourth of the fuel element length is roughened to enhance the heat transfer.

Reducing the number of fuel pins per element does not affect significally the volume fractions of the design. A set of fixed design parameters used in the study is described in table 1.

Table 1 Fixed design parameters

	oxide fuel	carbide fuel
core height	1.4 m	1.2 m
system pressure	90 bars	90 bars
core pressure drop	3 bars	3 bars
core inlet temp.	280°C	280°C
stanton number multiplier	2.5	2.5
fraction of theoretical density	85 %	80 %
number of core regions occupying equal volume	4	4
cladding material	SS 316	SS316

Pin Diameter. 3a - 3d

Varying the pin diameter the same trend was realised in both fuels. With fixed values of maximum fuel and cladding temperature, of core pressure drop and pin height, an increase in the pin diameter results in low enriched designs with large fuel volume fraction and reduced specific power ratio (watts/kg fiss.)

The maximum linear rating increases linearly with the pin diameter. The fact that the pin cross-section increases with the square power of the pin diameter and the coolant passage per pin is linearly increasing due to higher power production per pin, while the number of fuel pins required is linearly decreasing, results in linear core volume increase with the pin diameter. For the same reasons the fuel volume fraction is increasing linearly. The increased fuel volume fraction and core dimensions require low enriched fuel to get a critical system due to the decreased system leakage.

The upper limit of the pin diameter is determined from the neutronic properties of the resulting design. Thick pins with a higher fertile material concentration result in core conversion ratios close to one, which means increased reactivity with time. The lower limit is specified from technological and economic considerations such as the cladding fabrication and fuel cycle cost.

Fig. 3a-3d compare the variation of the most important design parameters for mixed oxide and mixed carbide fuels

Pin diameter

Fig. 3a

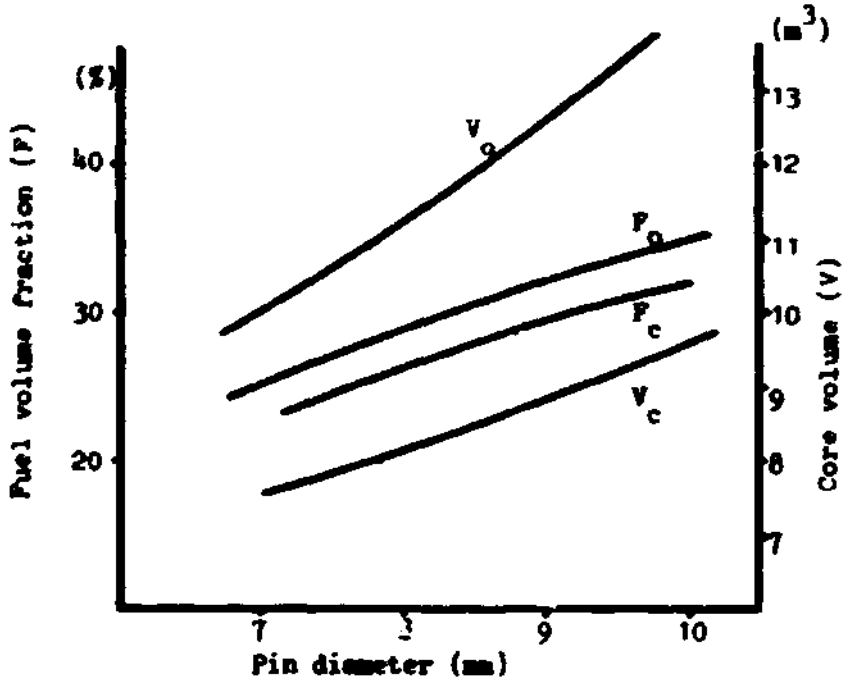

Fig. 3b

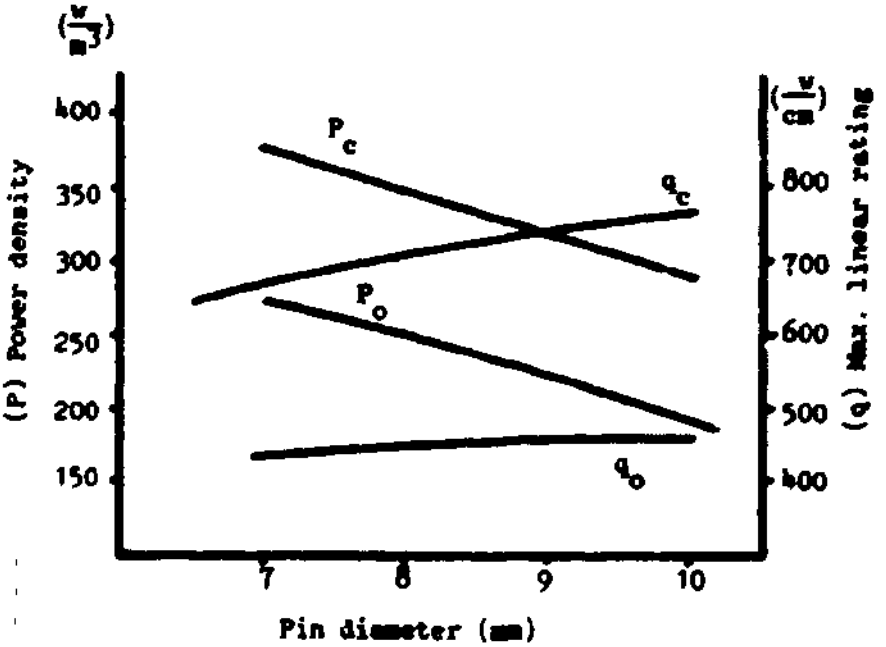

Fig. 3c

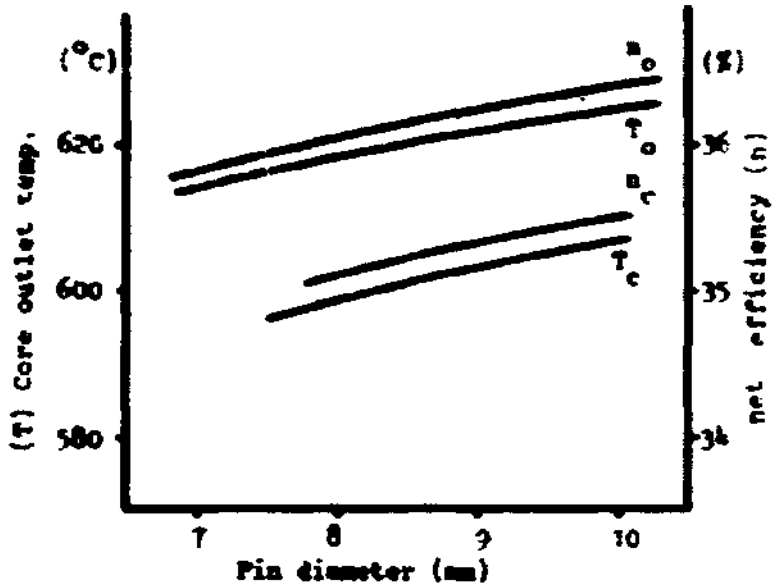

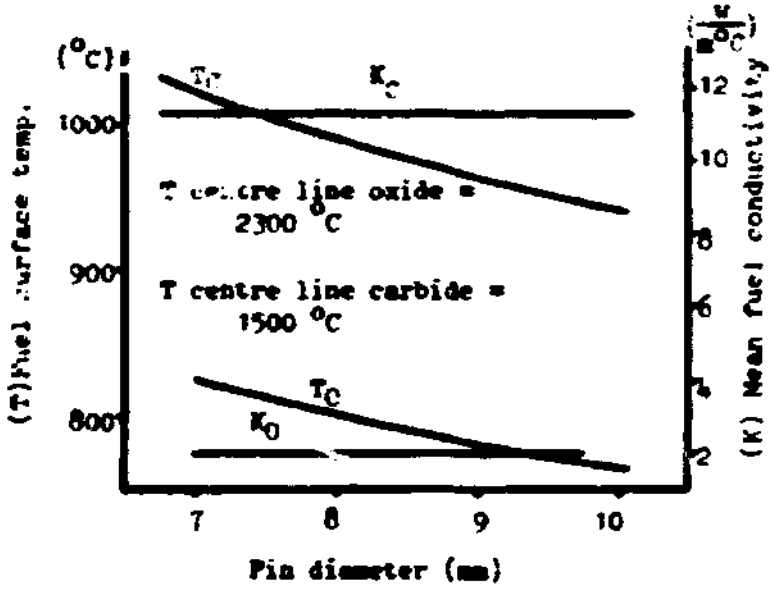

Fig. 3d

The parametric variation of the other independent variables concerns only the carbide fuel and shows the potential of a GCFR to utilise high heat conductivity fuels at high specific power densities.

These designs have not been studied in detail since they assume low fuel residence time, which is required by using present material limitations.

Core pressure drop. Fig. 4

If the temperature limits and the pin dimensions are fixed, a quite interesting influence is realised when the core pressure drop is varied (or the coolant velocity). Higher coolant velocity results in a reduced coolant passage per pin, since the pin power remains constant. For this reason the fuel volume fraction, and the breeding is increased. The disadvantage of such variation is a penalty in the plant efficiency due to losses in pumping power (see also fig. 2).

Core pressure drop Fig. 4

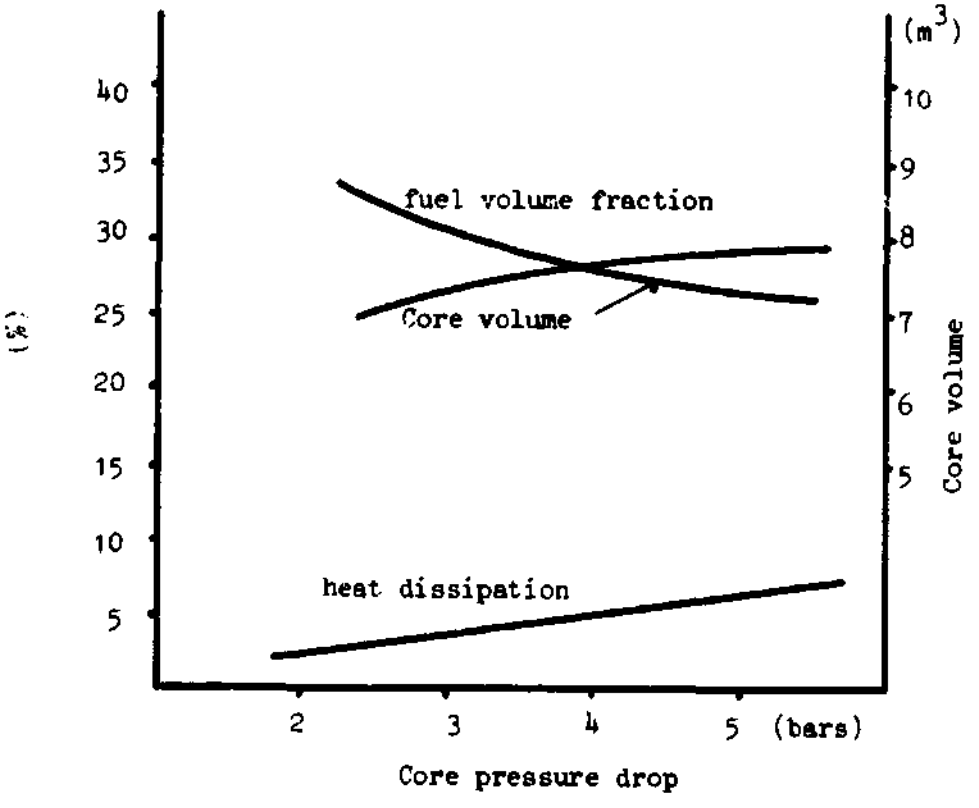

Core active height, Fig. 5a, 5b.

Again the temperature limits, the core pressure drop and the pin diameter is fixed. The increased core height results in higher core volume at lower fuel volume fractions and almost constant fuel enrichment.

The power produced per pin follows the increase in the pin height, since the linear power rating remains constant. Thus the total volume occupied by pins is constant.

The coolant passage per pin is increasing, firstly because the mass flow power pin should follow the pin power and secondly because the coolant velocity decreases in order to keep constant pressure drop at higher pin length. The increased coolant passage per pin results in lower fuel volume fraction, and higher coolant volume. The total core volume increases linearly with the pin length following the coolant passage variation or the power produced per pin.

The fuel enrichment remains rather constant since the leakage produced by the coolant fraction increase is compensated by the increase in the core dimensions.

Fig. 5a

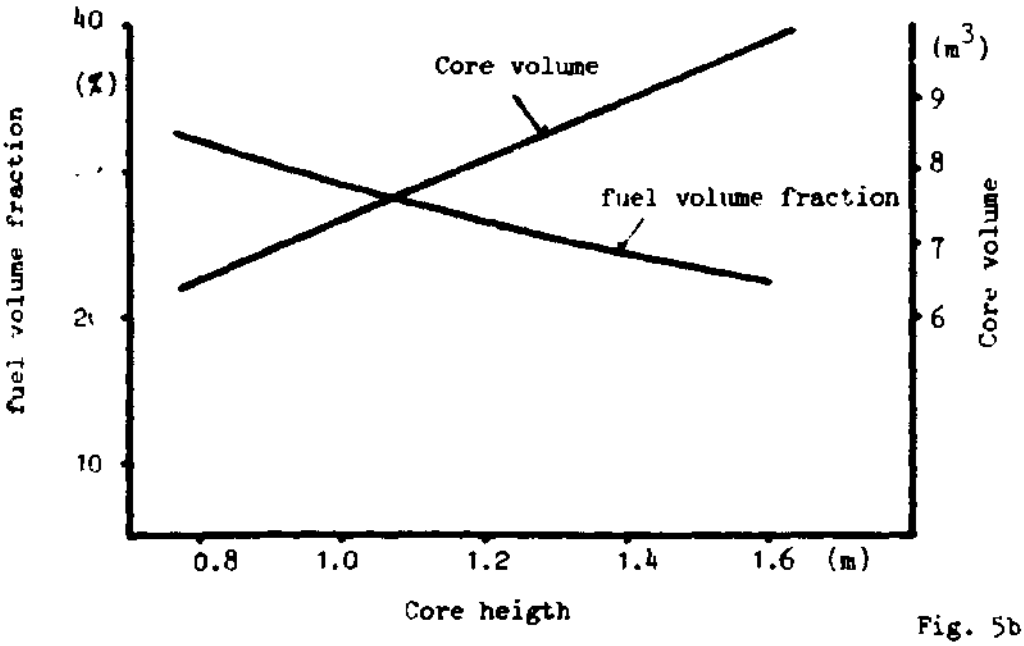
Core height
40
(%)
Core volume
fuel volume fraction
(m3)
9
8
7
6
Core volume
fuel volume fraction
20
10
0.8
1.0
1.2
1.4
1.6
(m)
Core heigth

Fig. 5b

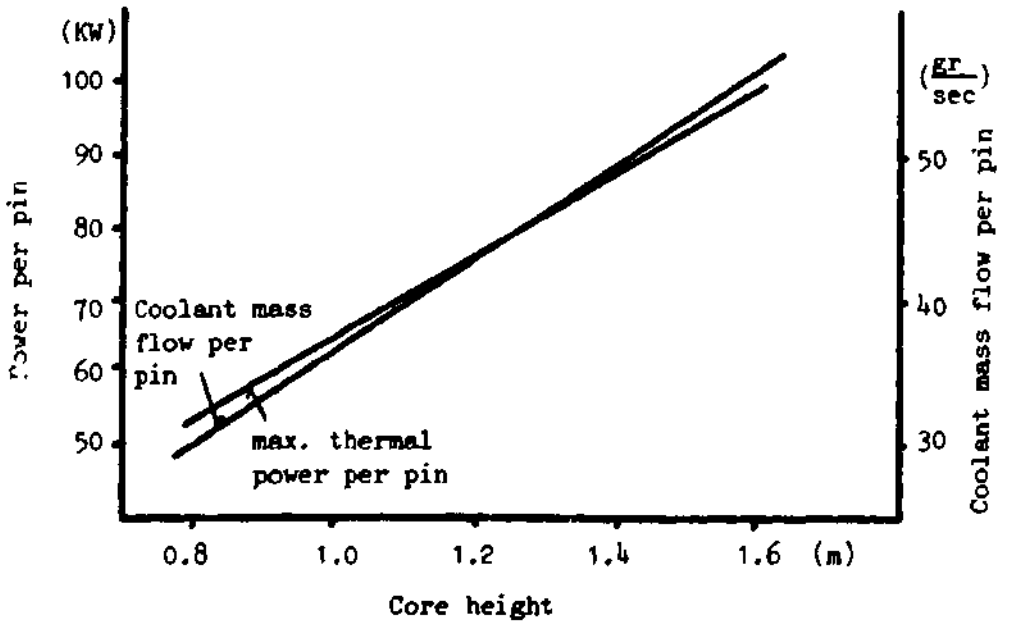
(KW)
100
90
80
70
60
50
Power per pin
Coolant mass flow per pin
max. thermal power per pin
(gr/sec)
50
40
30
Coolant mass flow per pin
0.8
1.0
1.2
1.4
1.6
(m)
Core height

Maximum cladding temperature, Fig. 6a - 6b.

With fixed pin dimensions, fuel centre line temperature and core pressure drop, a variation of the cladding temperature has the following consequences:

1) The core outlet temperature increases linearly with the cladding temperature. This improves the plant efficiency thus reducing the core dimensions for the same electrical power required.

2) The linear power rating decreases since the temperature difference between the fuel centre line and the surface is linearly reduced with cladding temperature.

This results in reduced coolant passage and in higher fuel volume fraction thus lowering the enrichment needed. Also the core volume is decreased (even with fixed thermal power) due to the reduction of the coolant fraction.

Fig. 6a

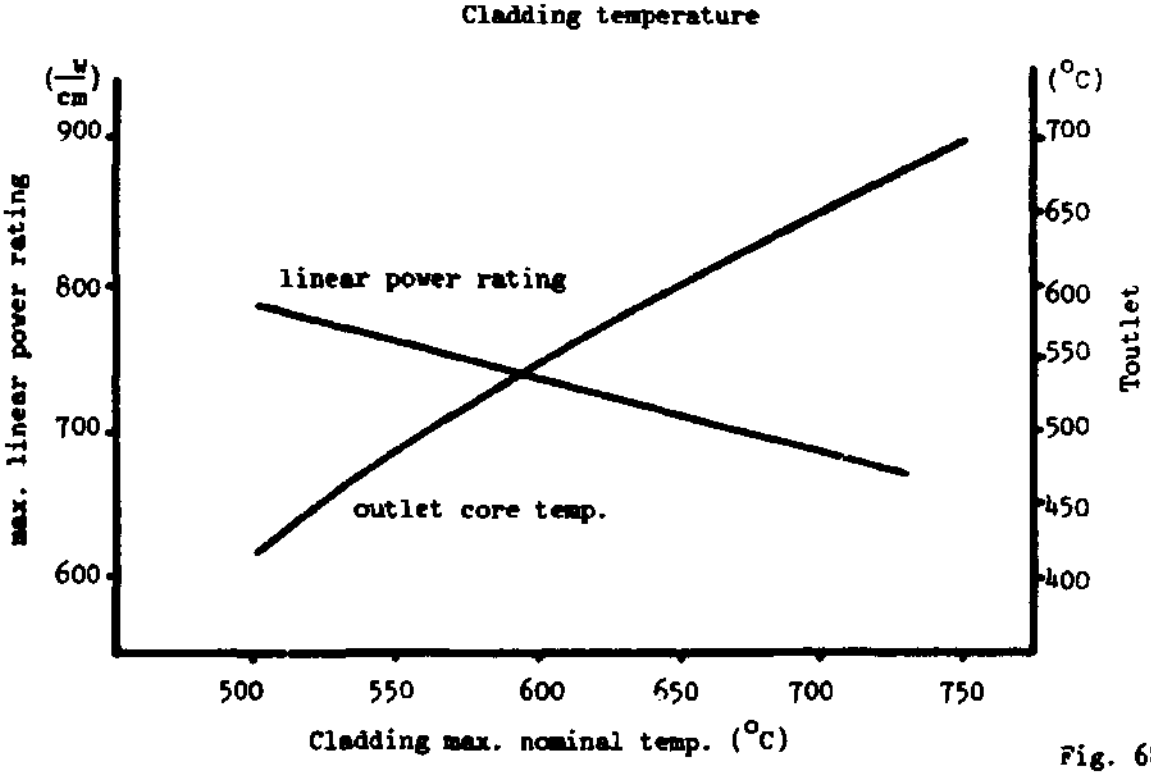
Cladding temperature
(W/cm)
900
800
700
600
max. linear power rating
(°C)
700
650
600
550
500
450
400
Toutlet
linear power rating
outlet core temp.
500
550
600
650
700
750
Cladding max. nominal temp. (°C)

Fig. 6b

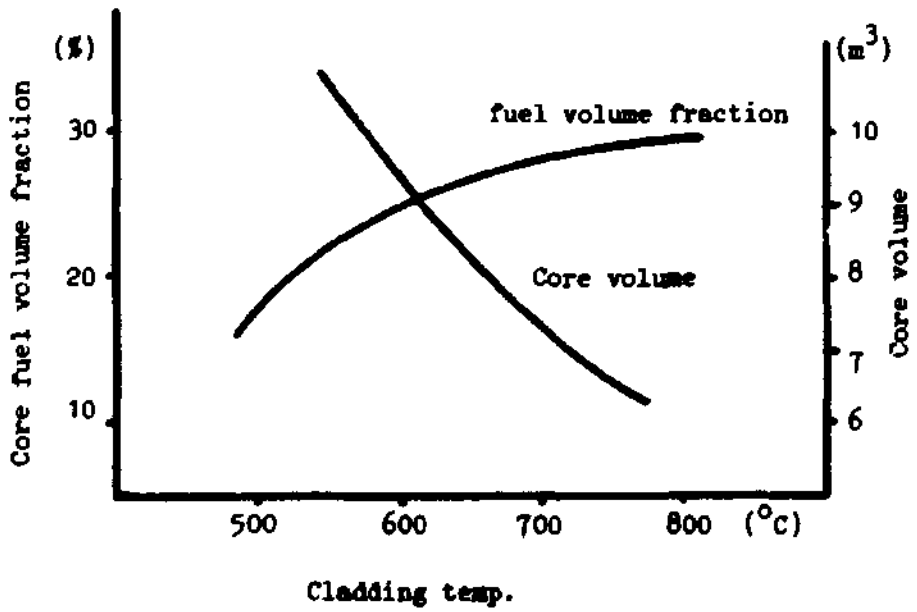
(%)
30
20
10
Core fuel volume fraction
(m³)
10
9
8
7
6
Core volume
fuel volume fraction
Core volume
500
600
700
800
(°C)
Cladding temp.

Maximum fuel centre line temperature, Fig. 7a - 7b.

The high value of carbide thermal conductivity permits values of maximum linear rating in the range of 800 watts/cm to 1300 watts/cm varying the maximum centre line temperature. This results in power densities two or three times higher than the oxide design, thus reducing the core volume and fissile Pu inventory.

The fuel volume fraction is reduced, increasing the linear rating due to the higher coolant passage per pin required, while highly enriched fuel must be used. The upper limit to the linear rating is determined from the fluence limit and economical considerations.

The fuel residence time is less than two years, due to high power density and the harder spectrum. Thus the fuel cycle cost penalty restricts the potential of the carbide fuel to utilise very high power ratings.

In GCFR's the core exit temperature is decreasing with increased linear power rating. With fixed core inlet conditions and maximum allowable cladding surface temperature the gas to cladding temperature difference follows the power rating and that lowers the gas temperature.

Thus an increase in the linear power rating from 450 w/cm to 700 w/cm results in 20°C core exit temperature reduction and 2.5 % lower efficiency (Fig 3b, 3c). The lower gas temperature effects also the heat exchanger surface.

In LMFBR's the disadvantage is not realised since to sodium heat transfer coefficient is five to six times higher to helium.

Maximum fuel centre line temperature

Fig. 7a

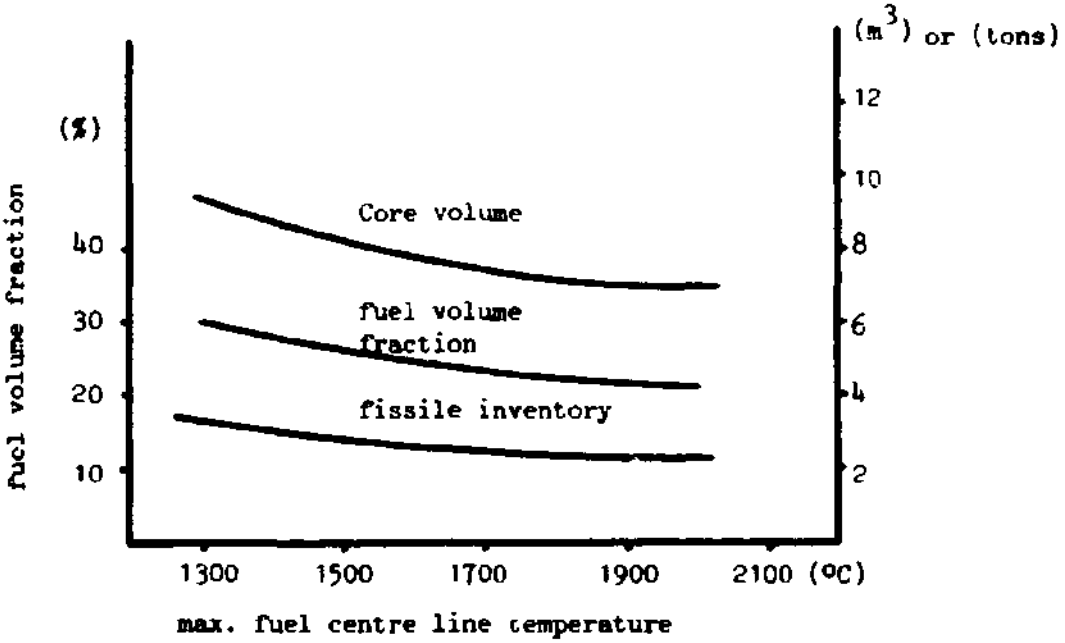

Fig. 7b

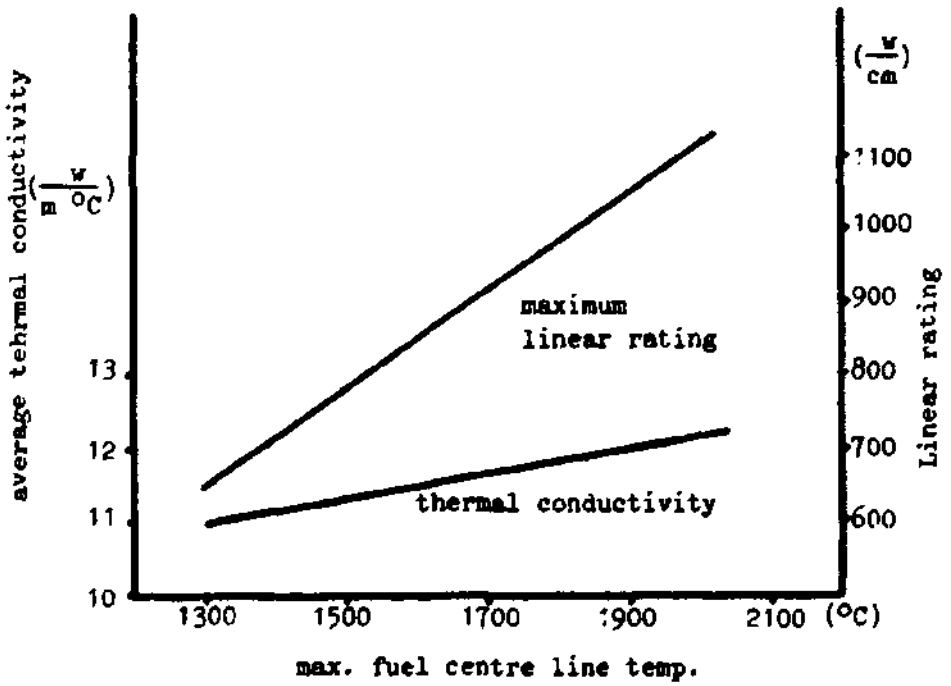

Comparative studies of mixed carbide versus mixed oxide fuel using the fuel management program GAUGEPM: Neutronic analysis and fuel cycle cost.

The designs described in fig. 3a - 3d were further analysed with GAUGEPM, covering the range between 7 mm to 10 mm in pin diameter. The results are given in fig. 8 and in tables 2, 3.

The spectrum calculations and the basic libraries and programs used are given in Appendix B. The calculation of fuel cycle cost follows the present worth method (3).

There are three basic components determining the fuel cycle cost. The net fissile material consumption per cycle, the fuel fabrication and the reprocessing expenses. The cost assumption as function of pin diameter are given in tables 2, 3.

The expenses and electricity revenues per cycle are discounted at the beginning of the cycle, to find the cycle cost, while the expenses and revenues of each cycle where discounted at the beginning of the reactor operation to find the levelised fuel cycle cost.

The mass balance per cycle, the breeding ratio and doubling time are calculated in the program. The definitions of breeding ratio and doubling time are in agreement with Wyckoff (4).

Residence times of 1.5 years - 3 years have been considered in the calculations, while the permissible residence time is given in fig. 9c.

It is not possible to achieve fuel residence times higher than two years with present cladding material limitations, although the carbide designs studied have a conservative power density. Two years residence time should be possible only using 10 mm diameter pin. This design uses low enriched fuel (11.2 %), a batch reloading scheme, with negligible reactivity swings and high plutonium fissile inventory (3.6 tons).

Comparing the fuel cycle cost of this design with the cost of the 8 mm oxide design indicates that there may not be an economic incentive to use mixed carbide fuel. The short fuel residence time will increase the fabrication and reprocessing expenditures and offsets the benefits of better breeding.

The need to improve the breeding performance of LMFBR's will provide the momentum for research and development work on carbide fuels and advanced structural and cladding materials. With these materials available fuel residence times of three years would be obtained. In this case optimum carbide designs in the range of 8 mm - 9 mm in pin diameter are possible. Their fissile inventory is in the range of 3 tons while compound doubling times of 8 years are obtained, with breeding ratios above 1.5.

A considerable fuel cycle cost difference is realised in favour of carbide fuel when designs with the same residence time are compared. On the other hand one could try to design mixed oxide designs with four years residence time to obtain similar fuel cycle cost.

Neutronic results

Fig. 8a

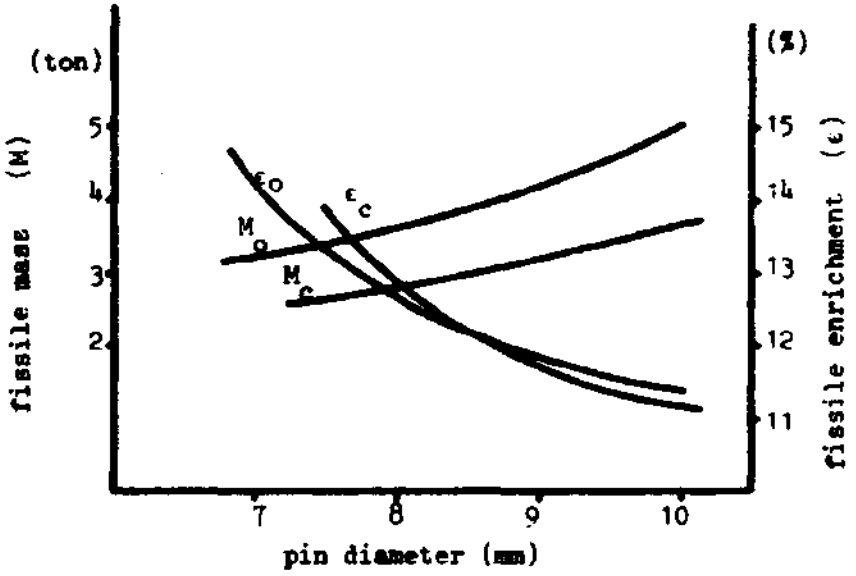

Fig. 8b

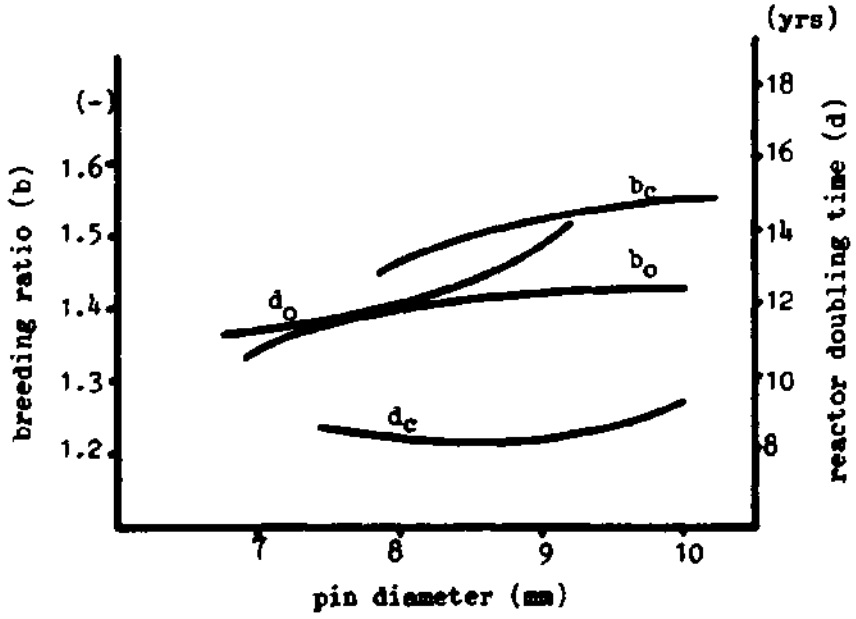

Fuel cycle cost results Fig. 9 a

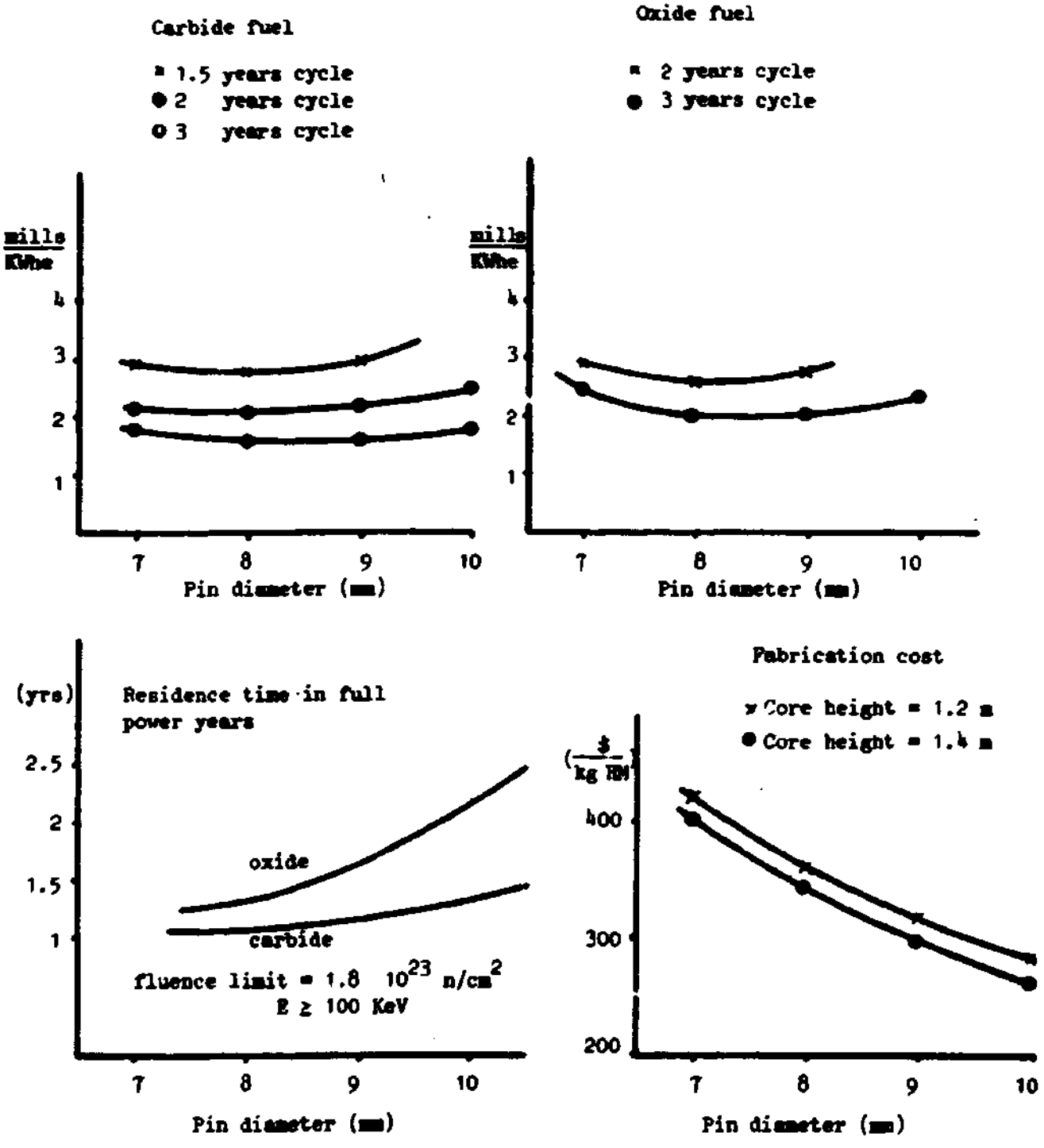

Tabel 2 - Mixed carbide fuel 1000 MWe

Core height = 1.2 m, T_{inlet} = 280°C, T_{fuel} = 1500°C, $T_{cladding}$ = 650°C, system pressure = 90 bar
core pressure drop = 3 bar, axial blanket = 60 cm, radial blanket = 37 cm, mean fuel conductivity 11 W
Heavy metal density 10.3 gr/cm^3, reprocessing cost = 200 $/kg, out of pile time = 1 year, radial blan
fabr. = 100 $/kg, fluence limit = 3.6 10^{23} n/cm^3, E > 100 KeV.

Pin diameter	mm	8	9	10.0
Core diameter	cm	294	307	320.3
Core volume	m^3	8.16	8.87	9.67
Fuel volume fraction	%	26.54	29.60	32.46
Mean enrichment	%	12.85	11.70	11.15
Fissile mass	kg	2800	3200	3650
Core outlet temp.	°C	599	603	607
Plant efficiency	%	35.12	35.32	35.50
Power density	w/cm^3	348	319	291
Linear rating	w/cm	710	740	767
Breeding ratio	-	1.46	1.52	1.54
Reactor doubling time	yrs	8.4	8.2	9.4
Fuel cycle cost (3 yrs cycle)	mills/kwhe	1.6	1.60	1.8
ΔK per year	%	1.8	.4	0.0
Core fabrication	$/kg	360	320	270
axial blanket fab. cost	$/kg	240	200	150
fuel residence time	yrs	2.2	2.5	2.9

Tab. 3 - Mixed oxide fuel 1000 MWe

Core height = 1.4 m, Tinlet = 280°C, Tfuel = 2300°C, Tcladding = 650°C, system pressure = 90 bar, core pressure drop = 3 bar, axial blanket = 60 cm, radial blanket = 37 cm, mean fuel conductivity 2 Heavy metal density = 8.7 gr/cm^3, reprocessing cost = 200 $/kg, fabrication of radial blanket = 100 of pile time = 1 year, fluence limit = 3.6 10^{23} n/cm^2, E>100 keV

Pin diameter	mm	7	8	9
Core diameter	cm	302.6	320.8	339.
Core volume	m^3	10.	11.32	12.66
Fuel volume fraction	%	25.3	28.89	32.14
Mean enrichment	%	14.25	12.6	11.4
Fissile mass	kg	3210	3600	4220
Core outlet temp.	°C	614.6	619.	622.
Plant efficiency	%	35.88	36.09	36.25
Power density	w/cm^3	277	245	218
Linear rating	w/cm	435	446	455
Breeding ratio	-	1.34	1.40	1.42
Reactor doubling time	years	11.4	12	13.6
Fuel cycle cost (3 years cycle)	mills/kwh e	2.5	1.9	2.
ΔK per year	%	2.5	1.	0.
Core fabrication cost	$/kg	400	340	300
axial blanket fab.cost	$/kg	280	220	180
fuel residence time	yrs	2.5	3.	3.3

Conclusions

The carbide fuel improves the flexibility of GCFR's.

Three to four times higher linear power ratings are possible with reduced fissile Plutonium inventory and compact core designs at high power densities. Also breeding ratios of 1.5 with compound doubling times below 8 years could be achieved. The breeding ratio could be increased to 1.6 using three row blankets.

Although liquid sodium is most appropriate coolant at high linear ratings, helium could work successfully at moderate power densities (400 w/cm^3), with comparable to mixed oxide design pumping power losses.

The disadvantage of designs with high power rating (which valids for both breeders) is their reduced fuel residence time and thus their increased fabrication and reprocessing expenses per cycle.

The use of carbide fuel in GCFR's would be desirable only with simultaneous introduction of advanced structural and cladding materials. Then it would be possible to obtain fuel cycles of three years and to utilise the excellent breeding performance of mixed carbide fuel at optimal economic conditions.

Final Remarks

The study covers part of the problems concerning the carbide design. Safety problems where not analysed due to the restricted time available. Two main difficulties appear using carbide fuel in GCFR's.

The effect of oxygen to carbon reaction was not analysed, although it is rather accepted that carbide fuel is incompatible with moist helium.

The loss of coolant accident requires special attention due to high power densities used, although the temperature margin between working carbide fuel temperatures in normal operation and the fuel melting point has been increased.

The specification of a reasonable power density remains an open problem and the optimisation study should be followed by detailed safety analysis to find out if there is any potential safety problem at higher power rating or if there is any additional safety margin, working at the same power rating as with oxide fuel.

Literature

1. R.C. Noyes et all
Optimum pin diameter for LMFBR carbide fuels
Nuclear Technology, August 1975

2. S. Kypreos
GAUGEFM: A multigroup diffusion program for fuel management operations
TM-ST-387, 15. 12. 75

3. S. Kypreos
FBCOST: A program to calculate the fuel cycle cost of fast breeders using the present worth method

4. H.L. Wyckoff, P. Greebler
Definitions of breeding ratio and doubling time
Nucl. Technology, March 74

Appendix A

Core thermohydraulics and neutronic calculations

Subroutine REGA (RE actor to GAs) calculates the temperature and pressure distribution in a helium cooled reactor with cylindrical fuel pins under certain constraints.

These constraints are the maximum fuel center line temperature and the maximum outside cladding wall temperature at a desired core pressure drop.

The basic assumption for the axial power profile is:

$$(1) \quad \frac{dQ}{dz} \equiv q(z) = q_m \cos\frac{\pi z}{L'} \quad , \quad -\frac{L}{2} \leq z \leq L/2$$

$$(2) \quad dQ = \dot{m}\, Cp\, dT \qquad\qquad L' = L + 2\delta$$

where q_m is the heat rate production per unit length at the mid plane (maximum linear rating) L is the core height, and δ the axial reflector savings.

The gas temperature distribution is calculated integrating eqs 1 and 2.

$$(3) \quad T_g(z) = T_{inlet} + \frac{q_m L'}{\dot{m}\, Cp\, \pi} (\sin wz_o + \sin wz)$$

$$w = \frac{\pi}{L'} \quad , \quad z_o = \frac{L}{2}$$

The coolant heat transfer coefficient is defined as:

(4) $a_{gas} = \frac{q\,(z)}{\Delta T(z)\ \pi d}$ where d is the pin diameter

and $\Delta T\,(z)$ is the cladding to gas temperature difference.

The cladding surface temperature is given by

(5) $T_c\,(z) = T_g(z) + \Delta T\,(z) = T_{inlet} + \frac{q_m\ L'}{\dot{m}\ Cp\ M}\ (\sin wz_o + \sin wz)$

$$+ \frac{q_m \cos wz}{\pi d\ a_{gas}}$$

The derivative of this expression defines the position (z_1) where the maximum surface cladding temperature occurs, and it can be proven that:

(6) $$\frac{T_{max,clad} - T_{inlet}}{T_{outlet} - T_{inlet}} = 1/2\ \left(1. + \frac{\sqrt{1. + ctg\ z_1^2}}{\sin wz_o}\right)$$

with $ctg\ wz_1 = \frac{\dot{m}\ c_p\ w}{\pi d\ a_{gas}}$

The gas heat transfer coefficient is given by:

(7) $a_{gas} = M_a \cdot \psi\ \frac{\dot{m} \cdot c_p}{F} \cdot 0.023 \cdot R_e^{-.2} \cdot P_r^{-.6} =$

(7)' $= k_w \cdot M_a \cdot \psi \cdot d^{.2} \cdot m^{.8} / F$ with

$$k_w = .02192\ \ \eta^{.2} \cdot P_r^{-.6}\ .\ C_p$$

M_a is the Stanton number multiplier used for roughened pins.

ψ is a correction factor which accounts for the fuel element geometry.

$$(8)\quad \psi = 1. + .912 \cdot Re^{-.1} \cdot Pr^{.4} \cdot (1. - 2.0043\, e^{-\bar{d}_h/d})$$

$$(9)\quad \bar{d}_h / d = \frac{4F}{\pi d^2}, \quad Re = \frac{\dot{m}}{F}\,\frac{d_h}{n}$$

$$(10)\quad n = 1.855 \cdot 10^{-5} \left(\frac{Tgas + 273.2}{273.2}\right)^{.68}$$

Relations (6) and (7.) could specify the mass flow required to cool the central channel at given $T_{max,\ clad}$ for any core outlet temperature and any coolant passage per pin (F).
The core outlet gas temperature is specified by the second constraint.
The fuel centerline temperature is given by a similar to (6) expression:

$$(11)\quad \frac{T_{max,\ fuel} - T_{inlet}}{T_{outlet} - T_{inlet}} = \frac{1}{2}\left(1. + \frac{\sqrt{1. + ctg\ wz_2}^{\,2}}{\sin wz_o}\right)$$

$$(12)\quad ctg\ wz_2 = \frac{\Delta T \cdot w \cdot \dot{m} \cdot c_p}{q_m}$$

ΔT is the temperature difference between the gas and fuel centerline, at the mid plane.

$$(13)\quad \Delta T = \frac{q_m}{\pi}\left(\frac{1}{d \cdot a_{gas}} + \frac{\ln HK}{2 \cdot \lambda_{cl}} + \frac{HK}{a_{gap} \cdot d} + \frac{f}{4k}\right)$$

HK is the outside to inside pin diameter ratio
λ_{cl} is the cladding conductivity
a_{gap} is the gap conductance

f is a factor accounting for the central fuel gap and $\bar{K}$ is the mean fuel conductivity.

The program modifies the T_{outlet} until to reach the maximum permissible fuel temperature.

Mean value of conductivity

The fuel conductivity is temperature dependent. From the heat conduction equation in cylindrical geometry and with the heat source constant in radial direction one could prove:

$$(14)\quad \int_{T_{surf}}^{T_{center}} K(T)\,dT = \bar{K}\,(T_{center} - T_{surf}) = \frac{q_m \cdot f}{4\pi} \quad \text{(at mid-plane)}$$

$$(15)\quad f = \begin{cases} 1 \text{ if } H = 0 \\ 1 - \dfrac{H^2}{1-H^2} \ln {}^1\!/_{H^2} \end{cases}$$

where H is the fuel gap to fuel pellet diameter ratio.

It is known that:

$$(16)\quad K_C\,(T) = a_c + b_c\,T$$

$$(17)\quad K_o\,(T) = d_o + \frac{b_o}{T}$$

where the subscript "c" and "o" refer to mixed carbide and mixed oxide respectively. The coefficients a and b are functions of the fraction of the theoretical density used in the pellet, see fig. 1.

Integrating equation (14) with $\Delta T_{fuel} = T_{center} - T_{surf}$.

we get:

$$(18)\quad \bar{K}_o = a_o + \frac{b_o}{\Delta T_{fuel}} \ln \left(\frac{\Delta T_{fuel}}{T_{surf}} + 1\right)$$

$$(19)\quad \ln \left(\frac{\Delta T_{fuel}}{T_{surf}} + 1\right) = \frac{a_o \cdot \Delta T_{fuel}}{b_o} + \frac{q_m \cdot f}{4\pi\, b_o}$$

$$(20)\quad \bar{K}_c = a_c + \frac{b_c}{2} (2\, T_{surf} + \Delta T_{fuel}) = \frac{q_m \cdot f}{4\pi\, \Delta T_{fuel}}$$

Equation (19) is solved with the Neutron's method for ΔT_{fuel}, while eq. (20) is directly solvable.

The fuel surface temperature at mid-plane is also known independently of $\bar{k}$.

$$(21)\quad T_{surf} = T_{inlet} + \frac{T_{out} - T_{inlet}}{2} + \frac{qm}{\pi} \left(\frac{1}{d \cdot \alpha_{gas}} + \frac{\ln HK}{2\lambda_{cl}} + \frac{HK}{a_{gap} \cdot d}\right)$$

With known values of ΔT_{fuel} and T_{surf} at midplane, the mean conductivity is computed and used in (13) and (12) to define the T_{outlet} which preserves the second constraint.

Core pressure drop

In the pressure drop calculation the accelaration losses the spacer and fuel element geometry and the fuel pin rougheness are taken into consideration.

The coolant fraction per pin (F), or the coolant velocity, is varied to obtain a desired pressure drop, if possible.

Core dimensions

After specifying the mass flow per pin and the coolant fraction the core geometry is defined. The heat produced in the central channel is:

$$(22)\quad Q_{max} = \dot{m} \cdot c_p \cdot (T_{out} - T_{inlet})$$

The total number of pins is given from the thermal power required to produce a given electrical output and the mean power produced per pin, while the mean pin power is given from the power form factor and the Q_{max}.
The assumed fuel element and control element geometry and the total number of fuel pins required define the core dimensions.

The radius of each enrichment zone is calculated assuming equal volume per zone.

Neutronic model

A one group synthesis model is used to specify the mean core enrichment and its distribution in the core regions in order to have a critical system with "flat" power profile. Iterations are provided between the neutronic and thermo hydraulic calculations over the power form factor.

Radial and axial calculation synthesis

In radial direction the one group diffusion equation is:

$$(23)\quad -\nabla D(r)\,\nabla\phi(r) + (\Sigma_a^c(r) + B_A^2(r))\,\phi(r) = \frac{\nu\Sigma^f(r)}{\lambda} \cdot \phi(r)$$

A difference method is applied to solve this equation in cylindrical geometry assuming a starting value of axial buckling (B_A). The calculated fluxes are used to compute the averaged core cross-sections,

$$(24)\quad \Sigma_e^c = \frac{\int_o^{core} \Sigma_e(r) \cdot \phi(r)\, r \cdot dr}{\int_o^{core} \phi(r)\, r\, dr}$$

while the radial buckling is given by the one group relation

$$(25)\quad \lambda = \frac{\nu \Sigma_f^c}{\Sigma_a^c + D^c (B_A^2 + B_R^2)}$$

The radial buckling is used in the axial calculations where the two region clab diffusion equation is analytically solved to give the transcendental equation:

$$(26)\quad B_A \frac{L}{2} \cdot \tan\left(B_A \frac{L}{2}\right) = \frac{L}{2} \cdot K \cdot \frac{D^b}{D^c} \cdot \coth(K \cdot \delta) \quad \text{with:}$$

$$(27)\quad K^2 = \frac{\Sigma_a^b - \nu \Sigma_f^b / \lambda}{D^b} + B_R^2$$

These equations are solved using the Newton's method to define a new value of axial buckling B_A. The new value of axial buckling is used again in the radial calculations (23) until to achieve a convergence.

The monoenergetic microscopic cross-sections could be calculated with GGC, as a function of U/P_u ratio, for a given buckling and fuel volume fraction, using the END7/B data files. Two outer iterations are provided.

One is modifying the mean core enrichment until to get a multiplication factor equal to a desired value (This partially compensates the systematic errors of the method).

The other iteration redestributes the region enrichment until to get equal power peaks per core region.

The algorith for this normalisation is:

$$(28)\quad e_{N+1}(i) = \cdot \left(\frac{\bar{P}}{P(i)}\right)^{1/2} \cdot e_N(i)$$

where $\bar{P}$ is the mean core power and P(i), e(i) the region peak power and enrichment respectively.

To avoid systematic error inherent to one group diffusion theory, the results of the above described approach are used as a first guess with the two dimensional diffusion multigroup program GAUGEFM to re-adjust for criticality and power normalisation taking into account burn-up reactivity losses. The multigroup program uses ENDF/B data condensed with MC2L.

Appendix B

Spectrum calculations

ENDF/B-3 data have been used with the programs ETOEL-MC2L (Los Alamos versions) to perform spectrum calculations and to produce the GAUGE libraries.

The inner cell region contains the fuel in average core composition, while its radius corresponds to the pellet radius. The outside region includes the cladding material and the coolant, while the radius concerns the core colume fractions. Fig. Ap. 1 gives the cell geometry used in MC2.

The fine group option was used with 12 nuclides and 1534 resonances.

Fig Ap 2 and Ap 3 give the energy distribution. Both spectra are similar. The medium energy of carbide is 210 KeV while for oxide fuel it is 170 KeV. Also the destructive flux of carbide is higher.

The harder spectrum of mixed carbide fuel is due to reduced moderation (one diluent atom for each heavy isotope) and the lower absorption cross-section of carbon.

The ENDF/B-3 data where condensed in 10 groups for detailed diffusion calculation and in four groups for fuel management.

Mixed oxide cell geometry

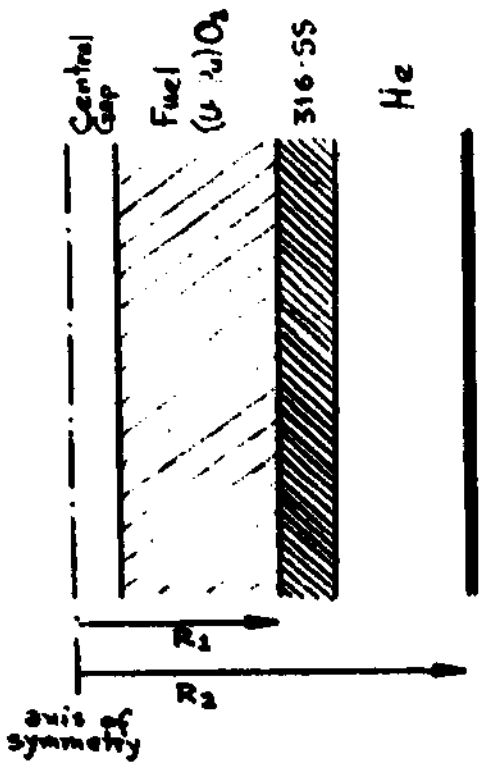

R_1 = .3261 cm
R_2 = .63796 cm

$\frac{\text{outside pin diameter}}{\text{inside pin diameter}}$ = 1.15

$\frac{\text{gap diameter}}{\text{inside pin diameter}}$ = .2

pin diameter = .75 cm

Fuel volume fraction = 25.12 % (region 1)
Stainless steel fract. = 14.32 % } (reg. 2)
Helium fraction = 60.53 % }

d_{ss} = 851.8·10^{-4} atoms/barn·cm
d_{HM}^{ss} = 220.0·10^{-4} "

Mixed carbide cell geomet

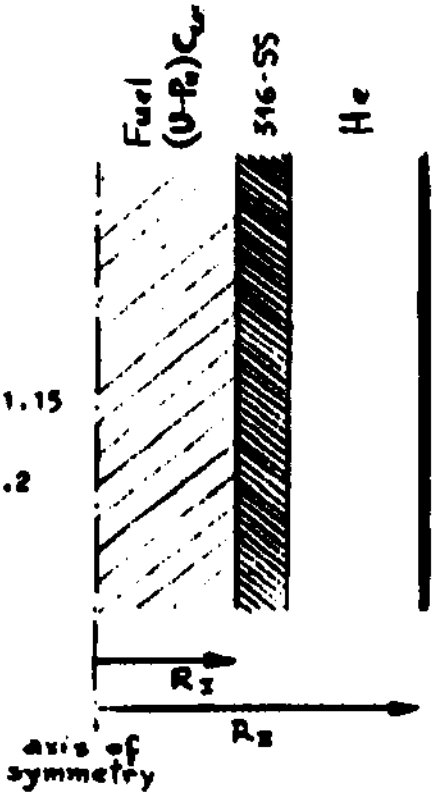

R_I = .3478 cm
R_{II} = .6277 cm

outside pin dia
inside pin diam

no central gap

pin diameter =

Fuel volume fraction = 30.74 %
Stainless steel fract. = 17.17 %
Helium fraction = 52.12 %

d_{ss} = 851.8·10^{-4} atoms/barn·cm
d_{HM} = 262.0·10^{-4} "

Isotopic composition

Stainless steel : Cr:.175, Mn:. 0.17, Fe:.645, Ni:.135, Mo:.028
Uranium : U-235:.0035, U-238:.9965
Plutonium : Pu-239:.8035, Pu-240:.1573, Pu-241:.0262. Pu-242:.013

Fig.Ap. 1: Cell geometries for spectrum calculations

Fig. Ap.2 Fraction of neutrons above a given lethargy
ENDF/B-3 MC2L fine group option

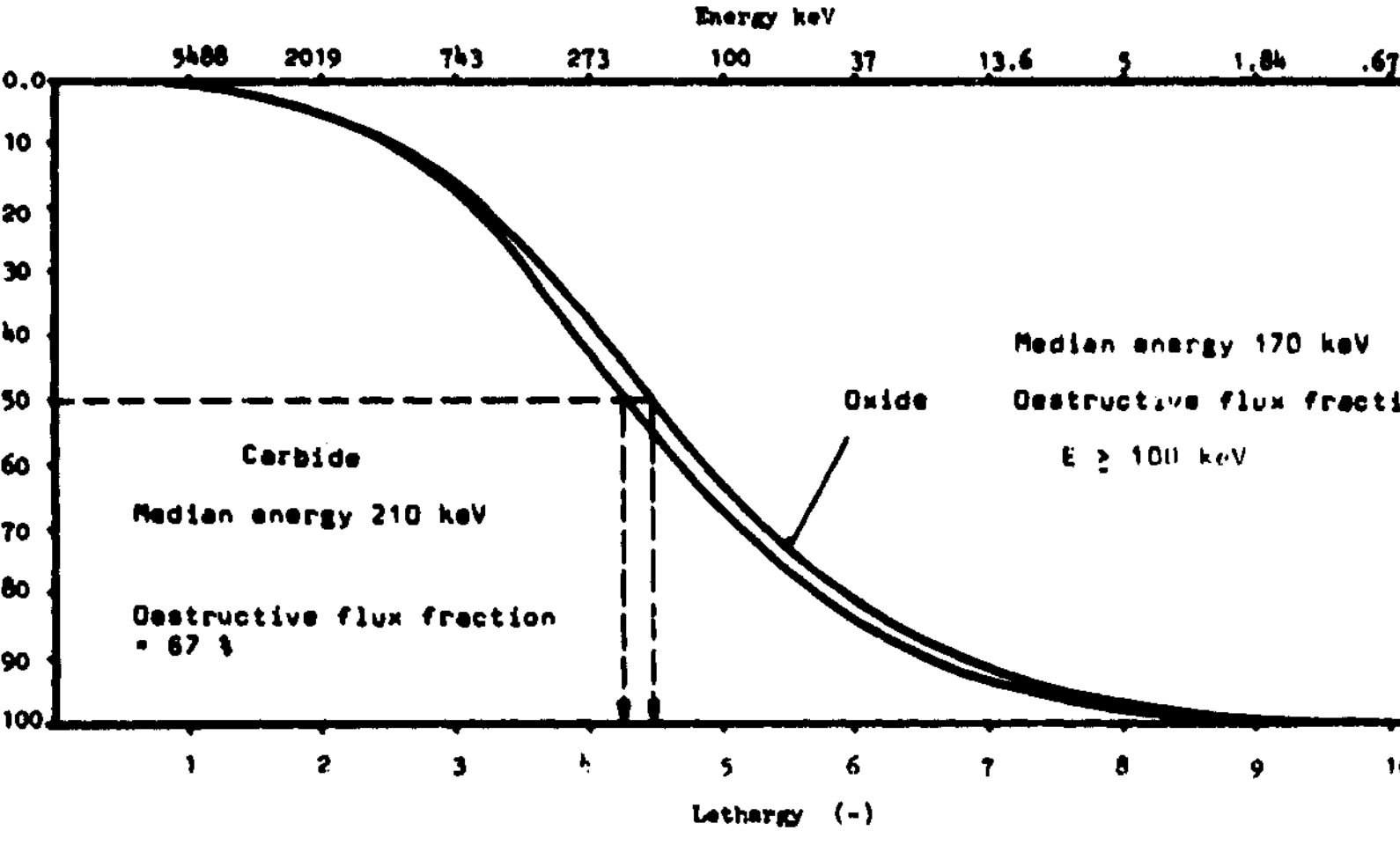

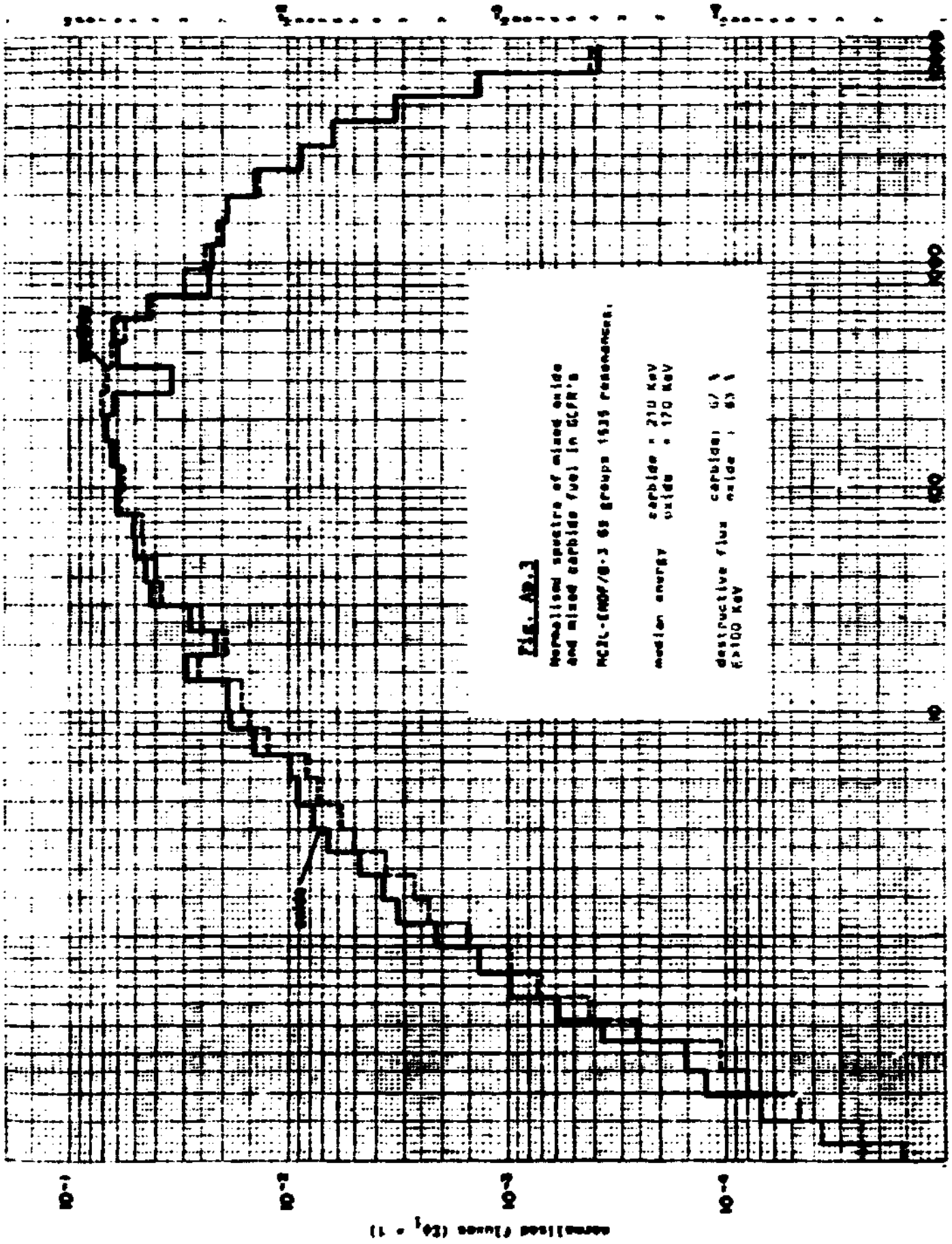
Fig. A2.3
Normalised spectra of mixed oxide and mixed carbide fuel in SCFR's
MCBC-EWDF/E-3 65 groups 1535 resonances.
median energy carbide = 210 KeV
oxide = 170 KeV
destructive flux carbide: 67 %
E>100 KeV oxide : 63 %
Energy (MeV)
accumulated fluxes (Σφ_i * 1)